Supplementary Information

Utilizing High Energy Photons via Energy Transfer for the Performance Enhancement of PTB7-Th:COi8DFIC Based Organic Solar Cells

Anoop C Sathyadevan Nair[a], *K P Adarsh Raj*[a], *Muneendra Dasannagari*[b], *Abhijith T*[c,d], *Abhishek Melarkode Rajendran*[a], *Dipangkor Basumatary*[a], *Safakath Karuthedath*[b*], *C. S. Suchand Sangeeth*[a]*, *Vari Sivaji Reddy*[a]*

[a] Department of Physics, National Institute of Technology Calicut (NITC), Kerala - 673601, India

[b] Institute of Materials Research, Tsinghua Shenzhen International Graduate School, Tsinghua University, Shenzhen – 518055, China

[c] Department of Physics, PSG Institute of Technology and Applied Research, Neelambur, Coimbatore, Tamil Nadu - 641062, India

[d] Department of Nanoscience and Technology, PSG Institute of Advanced Studies, Peelamedu, Coimbatore, Tamil Nadu - 641004, India.

*Corresponding authors

E-mail: sivaji@nitc.ac.in (Vari Sivaji Reddy)

E-mail: sangeeth@nitc.ac.in (C. S. Suchand Sangeeth)

E-mail: safakath@sz.tsinghua.edu.cn (Safakath Karuthedath)

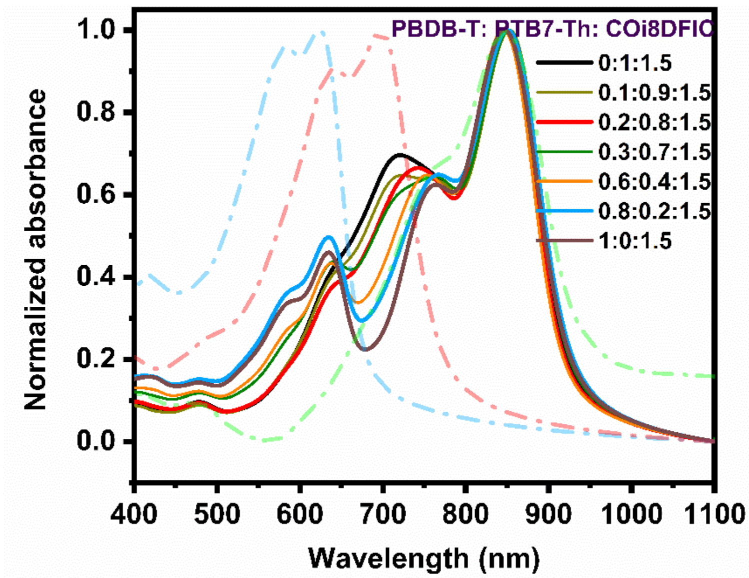

Figure S1. UV-Vis absorption spectra of active layer films at various PBDB-T:PTB7-Th weight ratios. The dotted lines represent the absorption spectra of pristine active layer molecules.

Supplementary Note:

The samples for UV-Vis absorption measurement was prepared by spin coating the solutions on precleaned glass substrates. Along with the absorption spectra of active layer blend films at various PBDB-T:PTB7-Th weight ratios, the spectra of pristine molecules are also provided in the background to get a clear picture of the peak positions. Pristine PBDB-T film exhibits an absorption peak at 623 nm, with a shoulder peak at 581 nm. For PTB7-Th, the main peak was found to be at 697 nm, with a shoulder peak at 637 nm. The non-fullerene acceptor COi8DFIC showed NIR absorption with peak at 847 nm and a shoulder peak at 760 nm. Each spectrum is normalized with respect to the maximum absorbance value. For the blend films, the highest peak around 850 nm is due to the large amount of COi8DFIC in the blend.

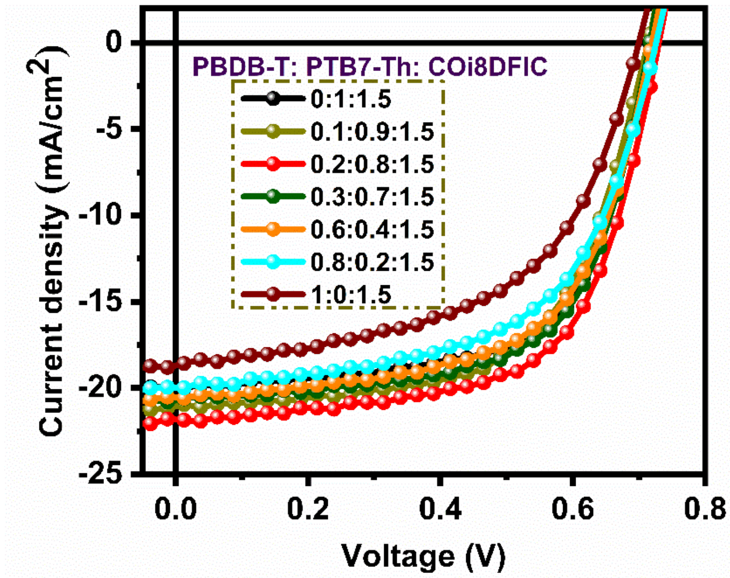

Figure S2. J-V characteristics of OSCs at various PBDB-T:PTB7-Th weight ratios.

Table S1. Photovoltaic parameters of OSCs with different PBDB-T:PTB7-Th weight ratios.

PBDB-T: PTB7-Th: COi8DFIC	J_{SC} (mA/cm^2)	V_{OC} (V)	FF (%)	PCE (%) Average	Best
0:1:1.5	19.86±0.67	0.721±0.003	61.93±1.81	8.87±0.24	9.16
0.1:0.9:1.5	20.28±0.57	0.715±0.004	62.13±1.34	9.01±0.14	9.24
0.2:0.8:1.5	21.36±0.36	0.726±0.004	62.80±0.48	9.74±0.17	9.98
0.3:0.7:1.5	20.63±0.38	0.716±0.008	62.36±0.76	9.20±0.15	9.44
0.6:0.4:1.5	20.41±0.33	0.717±0.004	59.08±1.87	8.65±0.28	9.01
0.8:0.2:1.5	20.05±0.43	0.721±0.006	56.31±1.11	8.15±0.15	8.34
1:0:1.5	18.15±0.37	0.708±0.006	52.91±1.04	6.81±0.13	7.06

Supplementary Note:

The I-V measurement of OSCs were carried out in the voltage range, -2 to 2 V by using a precision source/measure unit under 1 sun illumination. Before measurement, the intensity of the solar spectrum was calibrated by using a photo detector. Photovoltaic parameters were calculated from the J-V curve and average values were calculated from more than 9 devices.

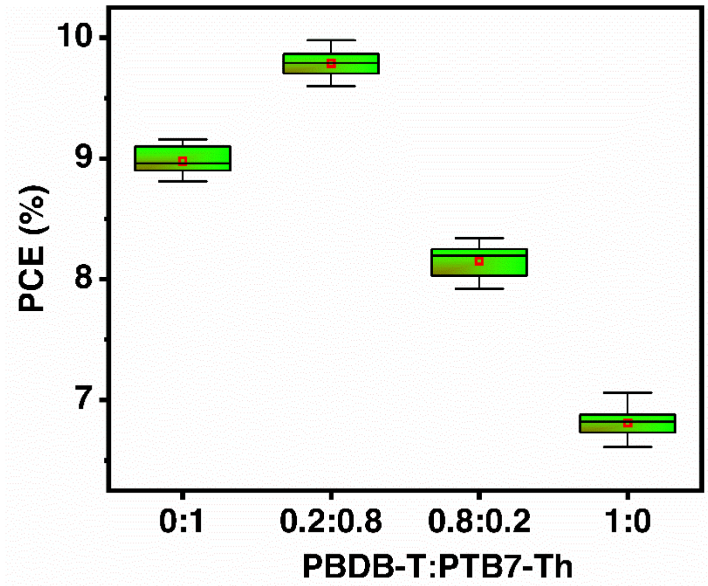

Figure S3. Box plots of PCE of OSCs fabricated with different PBDB-T:PTB7-Th weight ratio.

Supplementary Note:

Figure S3 presents the box plots of PCE of binary and ternary OSCs. It shows the mean, median, minimum and maximum values of PCE from each set. The compactness of the boxes and the whiskers confirms the reproducibility of the PCE values obtained.

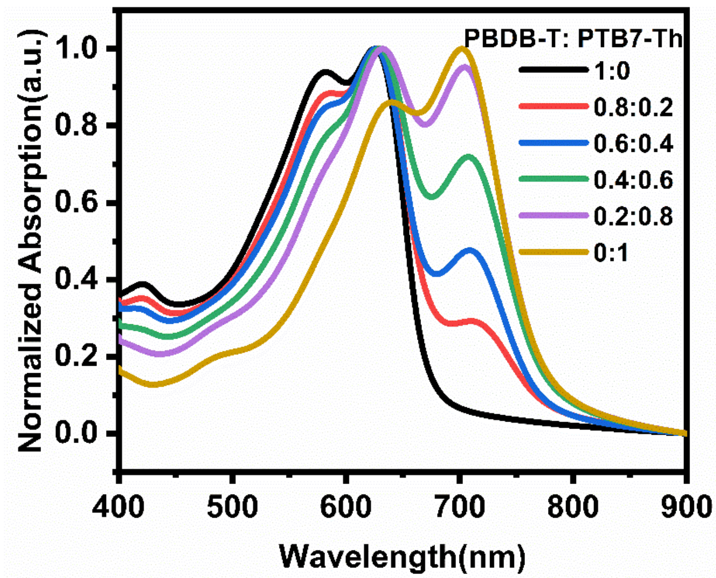

Figure S4. UV- Vis absorption spectra of PBDB-T: PTB7-Th blend films at various weight ratios.

Supplementary Note:

Figure S4 presents the normalized UV-Vis absorption spectra of PBDB-T:PTB7-Th blend films. The films were prepared on glass substrates from the same solutions which were used for steady state PL measurements. With increase in PTB7-Th content, a gradual increase in the PTB7-Th absorption intensity is observed in the blend film, validating the PBDB-T:PTB7-Th weight ratios in the samples used for PL measurement.

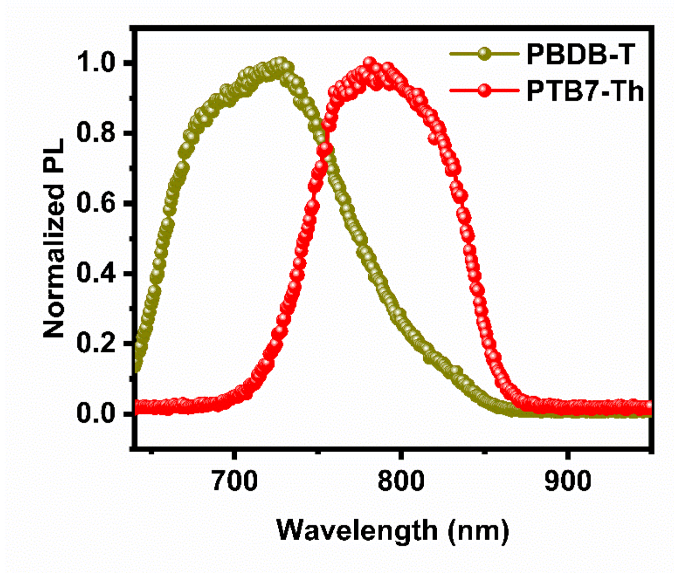

Figure S5. Normalized PL spectra of PBDB-T and PTB7-Th thin films.

Supplementary Note:

Figure S4 presents the normalized steady state photoluminescence spectra of pristine PBDB-T and PTB7-Th thin films. The samples were excited at a 620 nm wavelength. Both PBDB-T and PTB7-Th exhibited the emission peaks around 725 and 770 nm respectively. The decay profiles in TRPL measurements were monitored at these wavelengths.

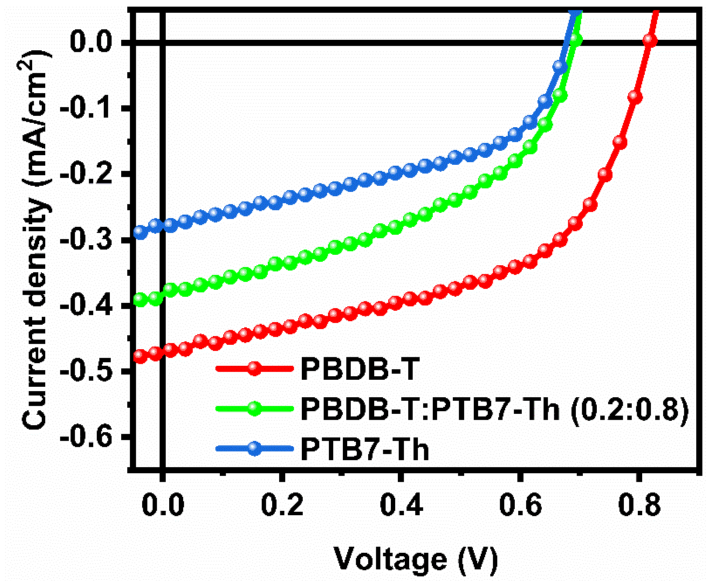

Figure S6. J-V characteristics of devices fabricated without COi8DFIC.

Supplementary Note:

To investigate the possibility of exciton dissociation at PBDB-T/PTB7-Th interface, devices were fabricated by using PBDB-T, PTB7-Th and PBDB-T:PTB7-Th (0.2:0.8) as the active layer (AL) with structure, ITO/ZnO/AL/MoO_3/Ag. If there is exciton dissociation at the PBDB-T/PTB7-Th interface, the J_{SC} of the device with blend as active layer will be more than that of the pristine donor-based devices. However, in the present study, the J_{SC} of the PBDB-T:PTB7-Th blend (0.38 mA/cm^2) was found to be in between the J_{SC} values of PBDB-T (0.47 mA/cm^2) and PTB7-Th (0.28 mA/cm^2) based devices, indicating negligible exciton dissociation at the interface.

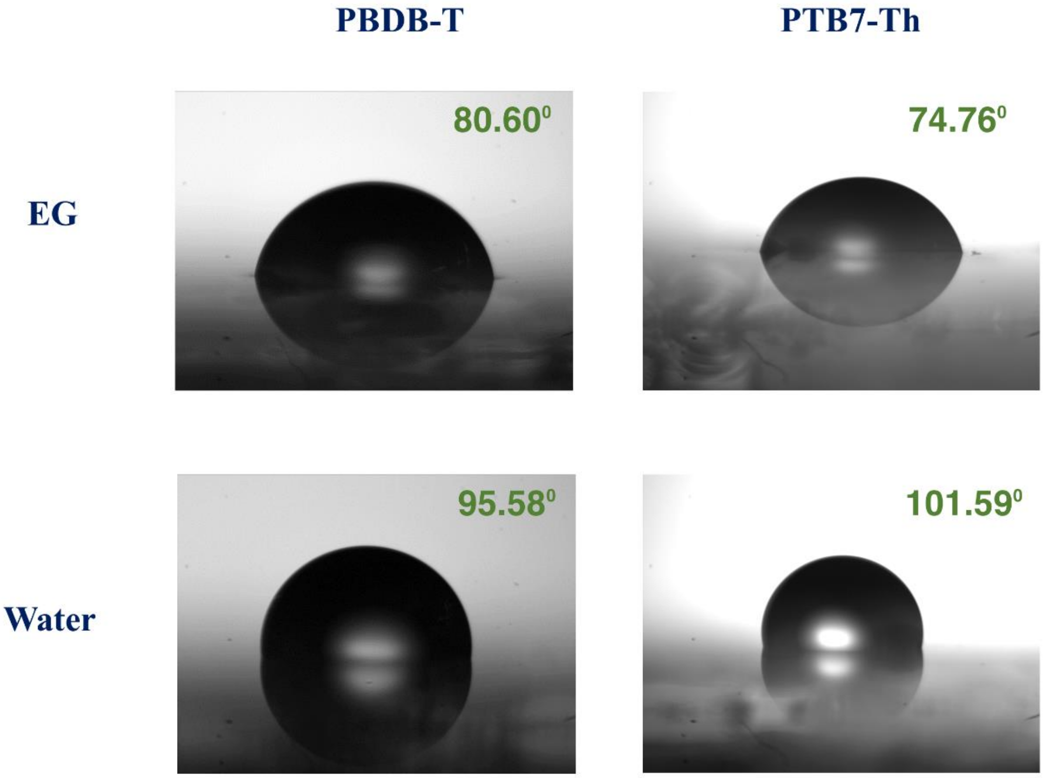

Figure S7. Water and ethylene glycol contact angles on pristine PBDB-T and PTB7-Th.

Supplementary Note:

The harmonic mean formula for calculating the surface energy of a material (γ_s) is given by,

$$\gamma_w(1+\cos\theta_w) = \frac{4\gamma_w^d\gamma_s^d}{\gamma_w^d+\gamma_s^d} + \frac{4\gamma_w^p\gamma_s^p}{\gamma_w^p+\gamma_s^p} \quad (1)$$

$$\gamma_{eg}(1+\cos\theta_{eg}) = \frac{4\gamma_{eg}^d\gamma_s^d}{\gamma_{eg}^d+\gamma_s^d} + \frac{4\gamma_{eg}^p\gamma_s^p}{\gamma_{eg}^p+\gamma_s^p} \quad (2)$$

By solving these two equations, γ_s^d and γ_s^p were obtained. The total surface energy is given by,

$$\gamma_s = \gamma_s^d + \gamma_s^d \quad (3)$$

Here, θ_w and θ_{eg} are the water and ethylene glycol contact angles.

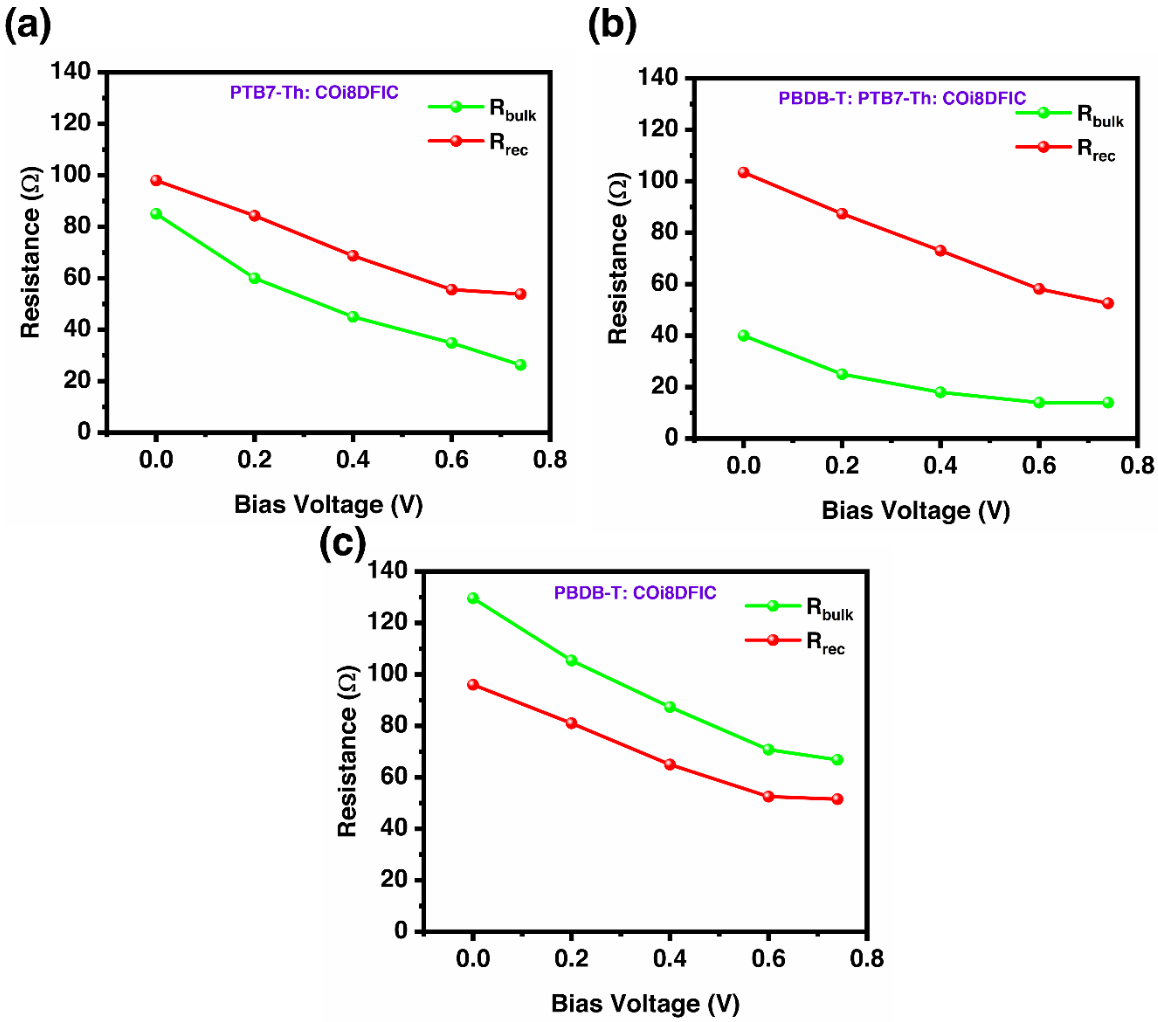

Figure S8. Variation of bulk and recombination resistances of (a) PTB7-Th:COi8DFIC, (b) PBDB-T:PTB7-Th:COi8DFIC and (c) PBDB-T:COi8DFIC based OSCs with bias voltage.

Supplementary Note:

Figure S6 shows the variation of bulk and recombination resistances of individual devices with applied bias voltage. All plots are presented in the same scale, in order to clearly understand the nature of charge transport mechanism.

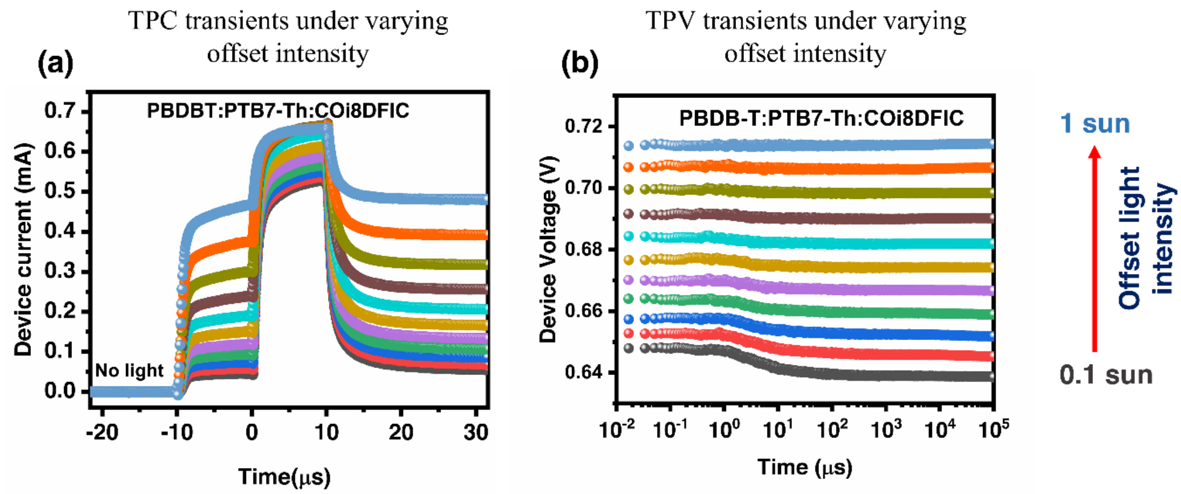

Figure S9. (a) Transient photocurrent and (b) photovoltage responses of optimal ternary OSC to a light pulse of 10 μs width, superimposed on varying offset light intensity which is varied from 0.1 sun to 1 sun.

Supplementary note:

Non-destructive TPC and TPV measurements were performed with Paios system[1]. A white light LED (400nm-780nm) with 15 μs pulse width superimposed on a constant bias light (varies from 0.1 sun to 1sun intensity) is applied on the device to create an additional charge which decays thereafter.

During TPC measurement, the device is kept at short-circuit condition and the photogenerated charge carrier response to the illuminated light pulse is shown in Figure S7 (a).

The decay profile gives charge extraction lifetime by fitting to the equation

$$I(t) = I_{SC} + \Delta I. exp\left(\frac{-t}{\tau_{TPC}}\right) \quad (1)$$

Where I_{SC} is the short-circuit current, ΔI is the additional current generated by light pulse, τ_{TPC} gives the extraction lifetime of free charge carriers[2,3].

During the TPV measurement, the device is kept at open-circuit condition, hence the charge generation is equal to recombination. Figure S7 (b) presents the TPV transients at various offset light intensities. The decay dynamics provides carrier lifetime by fitting to the equation,

$$V(t) = V_{OC} + \Delta V.exp\left(\frac{-t}{\tau_{TPV}}\right) \qquad (2)$$

Where, V_{OC} is the open circuit voltage, ΔV is increment in voltage due to light pulse and the τ_{TPV} minority carrier lifetime[4].

References

(1) Huang, Y.; Azeez, A.; Zhao, J.; Zhao, Z.; Dasannagari, M.; Laquai, F.; Kan, Z.; Karuthedath, S. Enhanced Device Performance through Optimization of Acceptor Layer Thickness Relative to Exciton Diffusion Length and Ionization Energy Offset in Bilayer Organic Solar Cells. *J. Mater. Chem. C* **2025**, *13* (11), 5911–5919. https://doi.org/10.1039/D4TC05190D.

(2) Sandberg, O. J.; Nyman, M.; Österbacka, R. Direct Determination of Doping Concentration and Built-in Voltage from Extraction Current Transients. *Org. Electron.* **2014**, *15* (11), 3413–3420. https://doi.org/10.1016/j.orgel.2014.09.027.

(3) Palomares, E.; Montcada, N. F.; Méndez, M.; Jiménez-López, J.; Yang, W.; Boschloo, G. Photovoltage/Photocurrent Transient Techniques. In *Characterization Techniques for Perovskite Solar Cell Materials*; Elsevier, 2020; pp 161–180. https://doi.org/10.1016/B978-0-12-814727-6.00007-4.

(4) O'Regan, B. C.; Lenzmann, F. Charge Transport and Recombination in a Nanoscale Interpenetrating Network of N-Type and p-Type Semiconductors: Transient Photocurrent and Photovoltage Studies of TiO_2 /Dye/CuSCN Photovoltaic Cells. *J. Phys. Chem. B* **2004**, *108* (14), 4342–4350. https://doi.org/10.1021/jp035613n.